GEOPHYSICS, VOL. 71, NO. 6 (NOVEMBER-DECEMBER 2006); P. V145–V152, 14 FIGS.
10.1190/1.2345050

DOI:10.1190/1.2345050

3D surface-related multiple elimination using parabolic sparse inversion

Ketil Hokstad[1] and Roger Sollie[1]

ABSTRACT

The basic theory of surface-related multiple elimination (SRME) can be formulated easily for 3D seismic data. However, because standard 3D seismic acquisition geometries violate the requirements of the method, the practical implementation for 3D seismic data is far from trivial. A major problem is to perform the crossline-summation step of 3D SRME, which becomes aliased because of the large separation between receiver cables and between source lines. A solution to this problem, based on hyperbolic sparse inversion, has been presented previously. This method is an alternative to extensive interpolation and extrapolation of data. The hyperbolic sparse inversion is formulated in the time domain and leads to few, but large, systems of equations. In this paper, we propose an alternative formulation using parabolic sparse inversion based on an efficient weighted minimum-norm solution that can be computed in the angular frequency domain. The main advantage of the new method is numerical efficiency because solving many small systems of equations often is faster than solving a few big ones. The method is demonstrated on 3D synthetic and real data with reflected and diffracted multiples. Numerical results show that the proposed method gives improved results compared to 2D SRME. For typical seismic acquisition geometries, the numerical cost running on 50 processors is 0.05 s per output trace. This makes production-scale processing of 3D seismic data feasible on current Linux clusters.

INTRODUCTION

A key factor of seismic data quality is the attenuation of multiple energy in the data. This is an issue for basically all seismic surveys, and the ability to handle unwanted multiples is important for subsequent imaging and amplitude analysis. With the increasing demand for extracting precise information from seismic data, the ability to solve the multiple problem will be even more important in the future. Seismic imaging techniques generally assume that the input data are free from multiples. Violating this assumption leads to spurious images and amplitudes. Some typical problems are (1) strong multiples masking subsalt reflections, (2) contamination of amplitude variation with offset (AVO) properties as a result of multiple energy, and (3) water-bottom multiples that coincide with the reservoir image. If multiples are not properly removed, they may be misinterpreted as or interfere with primary energy.

Surface-related multiple elimination (SRME) is, at least in principle, able to predict and attenuate all free-surface-related multiples. This method is data driven and does not rely on any simplifying assumptions regarding the subsurface. The basic idea underlying SRME was presented first by Kennett (1979), using a frequency-wavenumber (f-k) formulation for horizontally layered media. Berkhout (1982) generalized SRME to laterally inhomogeneous media, based on a feedback model. The frequently used adaptive formulation of SRME was presented by Verschuur et al. (1992) and Berkhout and Verschuur (1997). Alternative and equivalent formulations of SRME have been derived by Fokkema and van den Berg (1990) and van Borselen et al. (1996), based on the acoustic reciprocity theorem, and by Carvalho et al. (1991), based on an inverse scattering series. The practical issues of applying SRME to field data have been discussed by Dragoset and Jericevic (1998).

At present, 2D SRME is applied routinely by the seismic exploration industry. The extension of the basic theory to 3D seismic data is straightforward. However, the application of the method to 3D data acquired with current standard geometries is not trivial because basic requirements of the method are violated (van Borselen and Verschuur, 2003). A major reason for this is the large separation of source lines and receiver lines in the crossline direction.

A sparse inversion solution to the receiver-line problem has been formulated by van Dedem and Verschuur (2001, 2005). Using this method, multiple predictions can be performed using the available seismic data without extensive interpolation that expands the data volume prior to SRME. However, the numerical cost of this approach probably is still too high for large-scale production processing of 3D seismic data.

A practical 3D implementation of surface multiple attenuation is Shell's proprietary MAGIC3D code (Biersteker, 2001). In this im-

Manuscript received by the Editor October 4, 2004; revised manuscript received April 11, 2006; published online October 11, 2006.
[1]Statoil Research Centre, N-7005 Trondheim, Norway. E-mail: kehok@statoil.com; rsol@statoil.com.

DOI:10.1190/1.2345050

plementation, recorded shots are interpolated on the fly by interpolating the existing data sets. Thus, the computational efforts increase with the number of shots, and appropriate hardware is necessary. Application of this method to a real-size 3D data set has been presented by Kleemeyer et al. (2003).

In this paper, we present an implementation of 3D SRME, using the numerical scheme of Sacchi et al. (1998) to obtain an efficient weighted minimum-norm solution to the sparse-inversion problem formulated by van Dedem and Verschuur (2001, 2005). The present scheme was suggested first in an expanded abstract by Hokstad and Sollie (2003).

3D SRME

In the angular frequency domain, the 3D SRME method can be expressed as

$$P_0(\mathbf{g},\mathbf{s}) = P(\mathbf{g},\mathbf{s}) + \frac{R_0}{S(\omega)} \iint P_0(\mathbf{g},\mathbf{x})P(\mathbf{x},\mathbf{s})dx\,dy, \quad (1)$$

where $\mathbf{s}$ and $\mathbf{g}$ are source and receiver positions, P and P_0 are upgoing pressure with and without free-surface multiples, respectively, and R_0 is the reflection coefficient of the free surface. If the data are deghosted, $S(\omega)$ represents the spectrum of the seismic wavelet. The integral runs over the free surface $\mathbf{x} = (x,y,z = 0)$. We define x as the inline direction (i.e., sail-line direction) of the seismic survey and y as the crossline direction. To simplify the notation, we do not write the dependence upon angular frequency ω explicitly.

Equation 1 is an integral equation for the multiple-free wavefield P_0. For numerical implementation, equation 1 is discretized and expanded in a Neumann series (Verschuur et al., 1992) or formulated as an equivalent recursive process, as presented by Berkhout and Verschuur (1997). Moreover, it is convenient to split the multiple attenuation into two steps: multiple prediction and multiple subtraction. With these practical modifications, the 3D SRME method can be rewritten as an iterative procedure:

$$M^{(i)}(\mathbf{g},\mathbf{s}) = \sum_{y_k}\left[\sum_{x_k} P_0^{(i)}(\mathbf{g},\mathbf{x}_k)P(\mathbf{x}_k,\mathbf{s})\Delta x\right]\Delta y, \quad (2)$$

$$P_0^{(i+1)}(\mathbf{g},\mathbf{s}) = P(\mathbf{g},\mathbf{s}) - A^{(i)}(\omega)M^{(i)}(\mathbf{g},\mathbf{s}), \quad (3)$$

where $M^{(i)}$ is the 3D multiple prediction at iteration i, $\mathbf{x}_k = (x_k,y_k,0)$ is the discretized free surface, and Δx and Δy are the inline and crossline source and receiver spacings, respectively. The filter $A^{(i)}$ represents the inverse source spectrum. It can be applied locally in the time domain to account approximately for additional effects, such as lack of proper deghosting. In the first (and often only) iteration, P is substituted for $P_0^{(0)}$ on the right-hand side of equation 2. The term in brackets is a sequence of 2D inline multiple predictions. One of the major challenges of 3D SRME is to compute the crossline sum over y_k. Because of the large spacing of receiver cables and sail lines in 3D seismic acquisition, the crossline sum becomes seriously aliased.

PARABOLIC SPARSE INVERSION

The effect of the double sum in equation 2 is to extract the apex position of the kernel. Van Dedem and Verschuur (2001, 2005) show that the (aliased) crossline summation can be replaced by an inversion procedure, similar to a hyperbolic Radon transform, parameterized by intercept time, apex position, and curvature. This time-domain approach leads to few, but large, systems of linear equations. Numerically, it has the same drawbacks as the hyperbolic Radon transform presented by Thorson and Claerbout (1985). Today, the numerical cost is considered too high for processing real-size 3D seismic data volumes. Below, we suggest an alternative formulation based on a parabolic Radon transform in the angular frequency domain.

Like van Dedem and Verschuur, we use a Bayesian formulation of the inversion problem (Ulrych et al., 2001), with Gaussian likelihood and Cauchy prior distribution. For each source-receiver pair $\{\mathbf{s},\mathbf{g}\}$ and angular frequency ω, we define a data vector $\mathbf{d}$ with components

$$d(y_k) = \sum_{x_k} P_0^{(i)}(\mathbf{g},\mathbf{x}_k)P(\mathbf{x}_k,\mathbf{s})\Delta x, \quad (4)$$

where $k = 1,\ldots, N_d$, and N_d is the number of data points. Hence, $\mathbf{d}$ represents the inline part of the multiple prediction operator in equation 2. In the time domain, and for reflected events, van Dedem and Verschuur (2005) show that $\mathbf{d}$ has approximately a hyperbolic moveout T given by

$$T = \sqrt{\tau^2 + \frac{(y^0 - y_k)^2}{\hat{V}^2}}, \quad (5)$$

where τ is the intercept time, y^0 is the apex position, $\hat{V} \sim V_{\mathrm{NMO}}/2$, and V_{NMO} are the normal moveout (NMO) velocity. Expanding the moveout equation 5 in a Taylor series, we obtain the parabolic approximation

$$T \simeq \tau + q(y^0 - y_k)^2, \quad (6)$$

where $q = 1/2\tau\hat{V}^2$ is a curvature parameter. Because 3D surface seismic data are usually acquired with relatively small crossline offsets compared to target depth, we expect the parabolic approximation to be acceptable in most cases.

The discrete parabolic transformation from data space to model space can be expressed in the angular frequency domain as (Hampson, 1986; Schonewille and Duijndam, 2001)

$$m(q_i,y_j^0) = \sum_{k=1}^{N_d} d(y_k)\mathrm{e}^{-i\omega q_i(y_k - y_j^0)^2}\Delta y, \quad (7)$$

where the model space $\mathbf{m}$ is parameterized by the curvature q_i, $i = 1,\ldots, N_q$ and apex position y_j^0, $j = 1,\ldots, N_{y0}$. In matrix notation, we write

$$\mathbf{m} = \mathbf{L}^H\mathbf{d}, \quad (8)$$

$$\mathbf{d} = \mathbf{L}\mathbf{m}, \quad (9)$$

where $\mathbf{L}$ is an $N_d \times N_m$ matrix constructed from the complex exponential factors in equation 7 and $N_m = N_q N_{y0}$. The superscript H denotes the complex conjugate transpose.

The estimation of the model vector $\mathbf{m}$ can be posed as an inverse problem. Using a Bayesian approach to regularization, we are seeking a sparse solution where one, or a few, of the model parameters m_j are large and the others are close to zero. This is achieved using a Cauchy-distributed prior (Sacchi et al., 1998). With Gaussian likelihood and Cauchy prior (Gauss-Cauchy), the objective function to be minimized can be written as

DOI:10.1190/1.2345050

$$J(\mathbf{m}) = \frac{1}{2\sigma_n^2}(\mathbf{d} - \mathbf{Lm})^H(\mathbf{d} - \mathbf{Lm}) + C(\mathbf{m}), \quad (10)$$

where the regularizer imposed by the Cauchy distribution is given by

$$C(\mathbf{m}) = \sum_{j=1}^{N_m} \ln\left(1 + \frac{|m_j|^2}{2\sigma_m^2}\right). \quad (11)$$

The parameter σ_m^2 controls the sparseness of the solution. Computing the gradient of the objective function $J(\mathbf{m})$ with respect to $\mathbf{m}$ and equating to zero, the maximum a posteriori (MAP) estimator for the model vector $\mathbf{m}$ (Ulrych et al., 2001) is obtained as

$$\mathbf{m} = (\mathbf{L}^H\mathbf{L} + \lambda\mathbf{Q}^{-1})^{-1}\mathbf{L}^H\mathbf{d}, \quad (12)$$

where $\lambda = \sigma_n^2/\sigma_m^2$ and $\mathbf{Q}$ is an $N_m \times N_m$ diagonal matrix with elements

$$Q_{jj} = 1 + \frac{|m_j|^2}{2\sigma_m^2}. \quad (13)$$

Equation 12 is a weighted least-squares solution, which is applicable to overdetermined problems, i.e., when $N_d > N_m$ in equation 9. In 3D SRME of surface seismic data, the situation is the opposite: Typically, the number of data points per frequency is $N_d \sim 10$ and the number of model parameters $N_m \sim 500$, i.e., $N_d \ll N_m$.

Using the following matrix identity given by Sacchi and Ulrych (1995) and Sacchi et al. (1998),

$$(\mathbf{L}^H\mathbf{L} + \lambda\mathbf{Q}^{-1})^{-1}\mathbf{L}^H = \mathbf{QL}^H(\mathbf{LQL}^H + \lambda\mathbf{I})^{-1}, \quad (14)$$

where $\mathbf{I}$ is the identity matrix, equation 12 can be rewritten as

$$\mathbf{m} = \mathbf{QL}^H(\mathbf{LQL}^H + \lambda\mathbf{I})^{-1}\mathbf{d}. \quad (15)$$

Equation 15 represents a weighted minimum norm (or minimum length) solution, which is appropriate for underdetermined problems where $N_d < N_m$ (Menke, 1989).

The sparse solution in equation 15 is nonlinear because the matrix $\mathbf{Q}$ on the right-hand side depends on $\mathbf{m}$. It can be solved iteratively. Following Sacchi et al. (1998), we introduce an auxiliary vector $\mathbf{b}$ and compute

$$\mathbf{b}^{(n-1)} = (\mathbf{LQ}^{(n-1)}\mathbf{L}^H + \lambda\mathbf{I})^{-1}\mathbf{d}, \quad (16)$$

$$\mathbf{m}^{(n)} = \mathbf{Q}^{(n-1)}\mathbf{L}^H\mathbf{b}^{(n-1)}, \quad (17)$$

where n is the iteration number, which should not be confused with the SRME iteration index i in equations 2 and 3. In the first iteration, we replace $\mathbf{Q}$ by the $N_m \times N_m$ identity matrix. Then, the first iteration is equivalent to the solution with Gaussian distributions for both likelihood and prior (Gauss-Gauss). The small $N_d \times N_d$ matrix $\mathbf{LQ}^{(n-1)}\mathbf{L}^H + \lambda\mathbf{I}$ is Hermitian. The matrix inverse can be computed efficiently for each frequency using Cholesky decomposition. The main numerical cost, besides the matrix inversion, is the matrix-matrix multiplication $\mathbf{LQ}^{(n-1)}\mathbf{L}^H$ in equation 17 that must be recomputed at each iteration.

An important part of the iterative inversion scheme is to estimate the sparseness parameter σ_m^2 and update the matrix $\mathbf{Q}$. From a theoretical point of view, σ_n and σ_m are (stochastic) hyperparameters that should be estimated based on the data misfit in the objective function 10. For the current application, which involves processing large amounts of data, we have to choose a more practical approach. At each iteration, we compute the updates

$$\sigma_m^2 = \mu \times \max_k \left\{ \left(\frac{\sum_{i=1}^{N_w} |m_k^{(n)}(\omega_i)|}{N_\omega} \right)^2 \right\}, \quad (18)$$

$$Q_{jj}^{(n)} = 1 + \frac{(\sum_{i=1}^{N_w} |m_j^{(n)}(\omega_i)|)^2}{2N_\omega^2\sigma_m^2}, \quad (19)$$

where $0 < \mu < 1$ is a user-controlled parameter. Hence, a single matrix of weights $\mathbf{Q}$ is computed from all frequencies and applied to all frequencies. This averaging gives a smoothing effect that stabilizes the inversion scheme. The strategy given in equations 18 and 19 was proposed by Schonewille and Zwartjes (2002). A similar approach is used by Herrmann et al. (2000), but these authors use the model parameters $m_j(\omega_{k-1})$, obtained at frequency ω_{k-1}, to compute $\mathbf{Q}$ for the next frequency ω_k.

Finally, having obtained a sparse solution to the model-parameter vector $\mathbf{m}$, the multiple prediction $M(\mathbf{g},\mathbf{s})$ in equation 3 can be obtained by summation of the model parameters. Van Dedem and Verschuur (2005) have shown that

$$M(\boldsymbol{g},\boldsymbol{s}) = \sum_{j=1}^{N_{y0}} \sum_{i=1}^{N_q} F_c(q_i) m(q_i, y_j^0), \quad (20)$$

where F_c is an amplitude and phase correction derived in the stationary-phase approximation and given by

$$F_c(q_i) = \sqrt{\frac{\pi}{\omega q_i}} e^{-i\pi/4}. \quad (21)$$

SYNTHETIC DATA EXAMPLE

We generated synthetic 3D surface seismic data with free-surface multiples in a model consisting of three horizontal layers and a set of random point diffractors in the second layer, as shown in Figure 1.

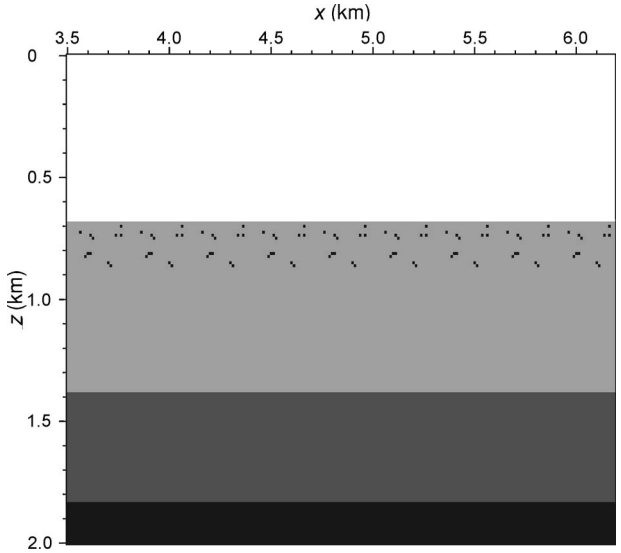

Figure 1. Vertical slice from the 3D diffractor model. The model has discrete translation invariance in both x- and y-directions.

The model has discrete translation invariance in the x- and y-directions such that

$$V_p(x + iD_x, y + jD_y, z) = V_p(x, y, z), \tag{22}$$

where V_p is the P-wave velocity, $D_x = 300$ m, $D_y = 250$ m, and i and j are arbitrary integers. Using high-order 3D finite differences, we modeled 10 source lines with 12 shots per line, totaling 120 shots. The source and receiver spacing in the numerical modeling was 25 m in both the inline (x) and crossline (y) directions. Because of the discrete translation invariance of the subsurface model, the 120 shot gathers can be used to simulate a 3D seismic survey of any desired size. Figure 2 shows the center receiver line, i.e., with zero crossline offset, from one of the raw synthetic 3D shot gathers. All features in the data that are not simple hyperbolic events are because of the random diffractors, including both diffracted primaries and diffracted multiples. The first-order ocean-bottom multiple appears at 1.9 s two-way time, with a tail of diffracted multiples following.

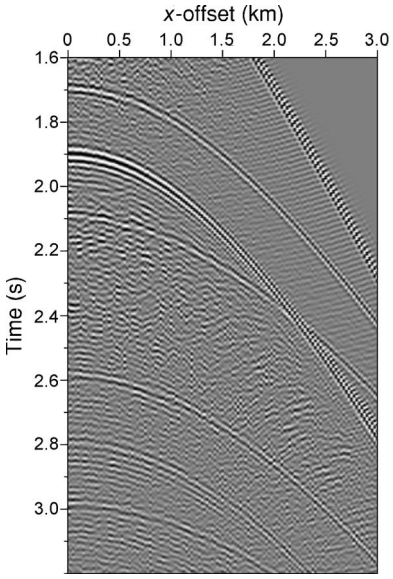

Figure 2. Center receiver line from an input 3D shot record with primaries, multiples, and diffractions. The first-order ocean-bottom multiple appears at 1.9 s two-way time.

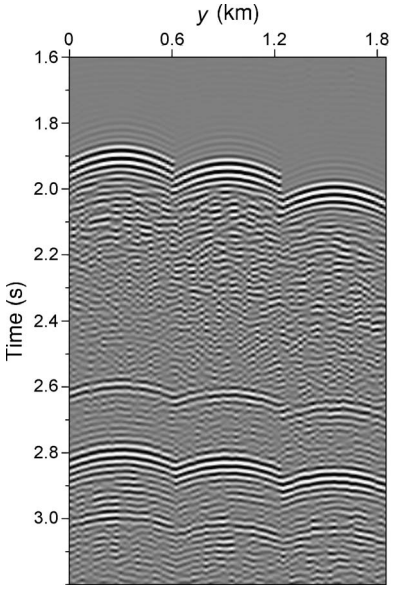

Figure 3. Intermediate crossline gathers after inline multiple prediction for 0.25-, 0.625-, and 1.0-km inline offset and zero crossline offset.

For comparison and reference, we applied 3D SRME to shot gathers with dense sampling of both sources and receivers. The shot gathers consist of 25 receiver lines with 121 receivers per line and with 25-m separation both inline and crossline. Simulated source lines with 25-m line spacing and 25-m source interval overlay each receiver line. The 3D SRME reference result was computed by brute summation in both inline and crossline directions. Figure 3 shows three intermediate crossline gathers after the inline multiple prediction on the center receiver line, corresponding to equation 4, transformed to the time domain. The 2D and 3D SRME lead to different results when the apex of the crossline gathers do not fall on the center receiver line. Figures 4 and 5 compare the predicted multiples and data after adaptive subtraction from 2D and 3D SRME, respectively. For these data, 3D SRME gives improved results compared to 2D SRME.

By decimation of the 3D finite-difference data set, we simulated an acquisition geometry with seven receiver lines per shot and

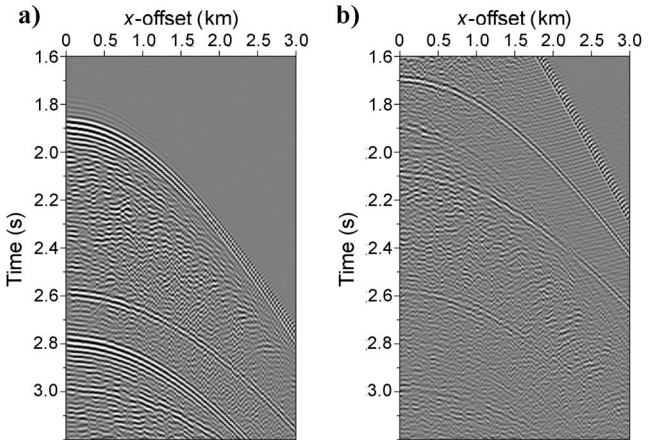

Figure 4. The 2D SRME result. (a) Predicted multiples and (b) after adaptive subtraction.

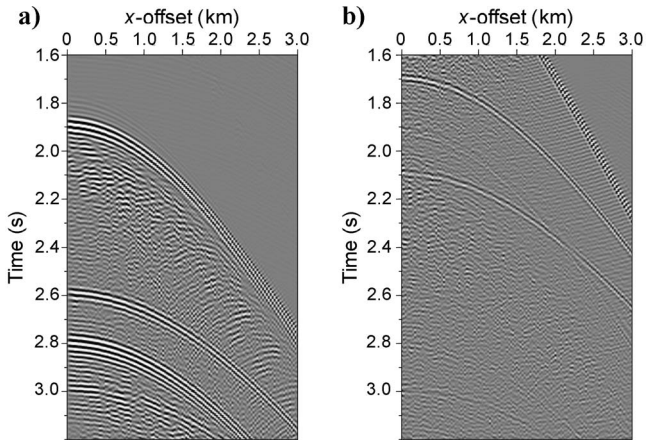

Figure 5. The 3D SRME reference with dense source and receiver sampling. (a) Predicted multiples and (b) after adaptive subtraction.

100-m source-line and receiver-line separation. In the inline direction, source and receiver spacing was 25 m. The 3D multiple prediction (equation 2) was performed by means of the sparse inversion scheme proposed above. The model space was spanned by $N_q = 30$ curvature parameters (omitting $q = 0$) with sampling $\Delta q = 0.1 \times 10^{-6}$ s/m^2, and $N_{y0} = 25$ apex offsets with sampling $\Delta y_0 = 25$ m, totaling $N_m = 750$ model parameters. The multiple-subtraction step (equation 2) was performed using the adaptive filter of Verschuur et al. (1992). The parameters of the adaptive filter were constant through all the numerical tests.

Figure 6 shows the result from 3D SRME with Gauss-Gauss inversion in the crossline summation, equivalent to the first iteration of the sparse inversion scheme. Gauss-Gauss inversion does not improve the multiple attenuation compared to the 2D SRME result in Figure 4. However, the diffracted multiples are attenuated better.

Figure 7 shows the result obtained after five iterations of the proposed Gauss-Cauchy sparse inversion scheme. The main multiple events are attenuated with better results than 2D SRME. However, some diffracted multiples remain in the data, compared to the 3D SRME reference in Figure 5. By means of numerical tests, we found that $\lambda = 0.03$ and $\mu = 0.1$ were good choices for the parameters controlling the sparse inversion (equations 15 and 18). The elapsed time for multiple prediction on one 3D shot gather was approximately 12 minutes, using eight processors on an SGI Origin 2000.

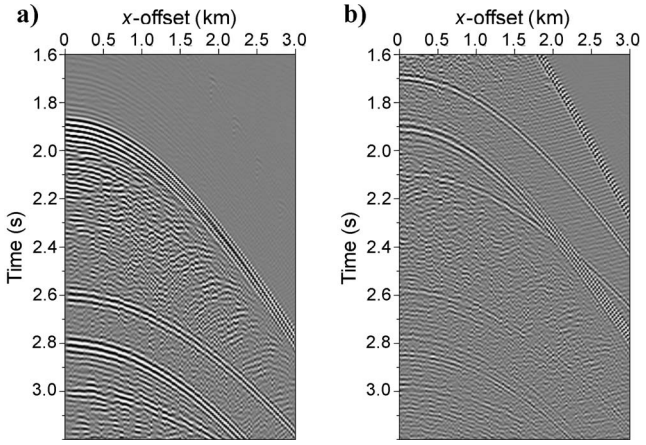

Figure 6. The 3D SRME with 100-m receiver-line separation and Gauss-Gauss inversion in the crossline summation. (a) Predicted multiples and (b) after adaptive subtraction.

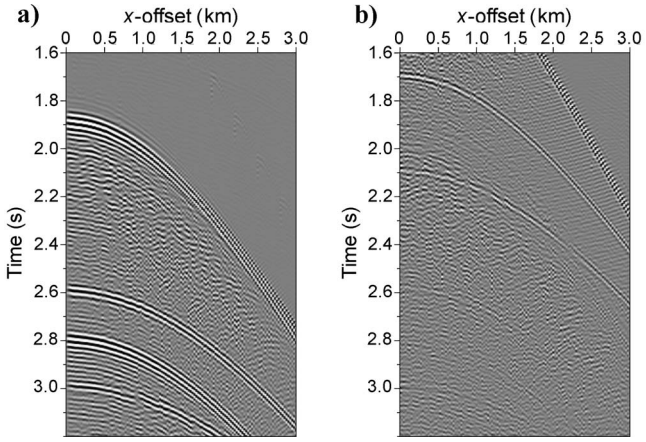

Figure 7. The 3-D SRME with 100-m receiver-line separation and five iterations of Gauss-Cauchy sparse inversion in the crossline summation. (a) Predicted multiples and (b) after adaptive subtraction.

REAL DATA EXAMPLE

The proposed 3D SRME method was applied to 3D surface seismic data acquired offshore of West Africa with four receiver lines and flip-flop sources. The multiple problems are severe, mainly from diffractors in the overburden. The data have a long processing and reprocessing record, using Radon demultiple and wave-equation-based methods as well as empirical random-noise attenuation techniques.

Figure 8 shows the source positions used in the 3D SRME example and the receiver lines for the first and last shot of each line. Free-surface multiples were predicted and subtracted from the center sail line. The two adjacent sail lines were used in the multiple prediction. We used 244 receivers with 25-m inline spacing from each receiver line. The nominal distance between receiver lines was 100 m. Each source line had 567 shotpoints with 25-m spacing. The distance between neighboring sail lines was 200 m. The nominal geometry is close to the theoretical requirement of coinciding source and receiver lines. The near offset was 110 m, and the water depth varies from 1150 to 1250 m, which corresponds to approximately 2.5° incidence angle at the ocean bottom. Consequently, data extrapolation to zero offset is not a major problem for this data set (compared to shallow water).

The sparse inversion parameters were set to the same values as in the synthetic example in the previous section, i.e., five iterations with $\lambda = 0.03$ and $\mu = 0.1$. The size of the model space was $N_q = 10$ and $N_{y0} = 17$, and the increments in model parameters were $\Delta q = 10^{-7}$ s/m^2 and $\Delta y_0 = 25.0$ m. The elapsed time for one output source line was 2 hours and 50 minutes, running on 16 processors on a 3.06-GHz Linux cluster. This elapsed time corresponds to approximately 0.02 s per predicted multiple trace (2048 samples per trace, 4-ms sampling, 1024 frequencies). The sparse inversion part of the numerical scheme accounts for approximately 85% of the computational cost, whereas the inline summation and data I/O [including fast Fourier transform (FFT)] contribute 10% and 5%, respectively.

Figure 9 shows the center receiver cable from one of the raw input 3D shot gathers. Figure 10 shows the predicted multiples and multiple-attenuation result for the same shot gather. A major part of the en-

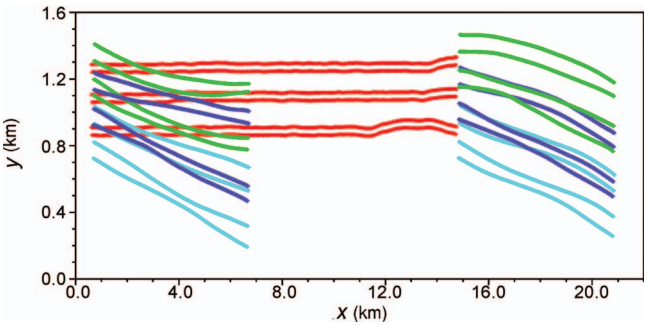

Figure 8. Source lines used in 3D SRME, and receiver lines for the first and last shot of each line. Data and images shown below correspond to the center sail line. Note that the scale of x- and y-axes is different.

ergy recorded after 3200- and 4200-ms two-way time is free-surface multiples, in particular, the first-order water-bottom multiple.

After the multiple attenuation, the center receiver lines were imaged by means of hyperbolic NMO correction, CMP stacking, and 2D poststack Kirchhoff time migration. Cable feathering degrades the performance of 3D SRME at large offsets. Therefore, the maximum offset used in the stack was 3000 m, and the CMP fold was 56. For comparison, we applied 2D SRME and imaging to the center receiver lines. Images were computed from raw input data, data after attenuation of free-surface multiples, and the multiples subtracted from prestack data. In all cases, we applied identical processing sequences, with the same CMP fold and velocity model.

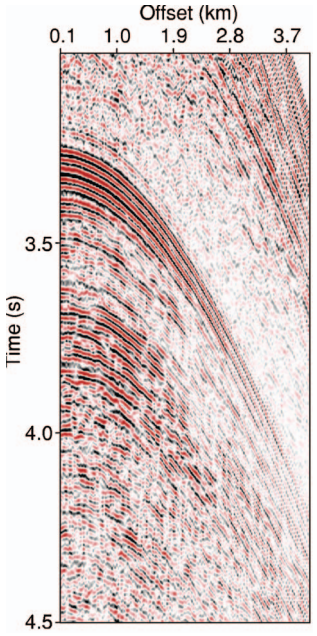

Figure 9. Center receiver lines from a 3D shot gather. Raw input data.

Figures 11 and 12 show Kirchhoff-migration images computed from the raw data, including both primaries and free-surface multiples, and after 3D SRME, respectively. The first ocean-bottom multiple can be observed at approximately 3.3 s two-way time, and the second ocean-bottom multiple is found near 5.0 s. Figure 13 shows a comparison of images obtained after 3D and 2D SRME. The result from 3D SRME is significantly better. Figure 14 shows, correspondingly, images computed from the subtracted multiples. Images of the multiples can be valuable for interpreters to identify residuals of free-surface multiples that remain in the image after multiple attenuation.

DISCUSSION

In principle, 3D extension of the SRME method is straightforward. In practice, a number of obstacles must be overcome because standard marine 3D seismic acquisition fails to meet the basic requirements of the method (Dragoset and Jericevic, 1998). Major challenges include (1) the large separation between receiver lines, (2) the large separation between source lines, (3) missing zero-offset data (theoretically, split-spread data are required), and (4) cable feathering from waves and ocean currents. Here, we only consider the problems related to the large distance between receiver lines in marine 3D seismic data. The corresponding source-line separation problem, which increases with the number of receiver cables and may be equally important, is addressed by Hokstad and Sollie (2004).

Van Dedem and Verschuur (2001, 2005) show that the events after inline multiple prediction as a function of crossline offset can be approximated by a hyperbolic traveltime equation. These authors introduce the sparse inversion approach to 3D SRME and propose a hyperbolic scheme related to the hyperbolic Radon transform. The

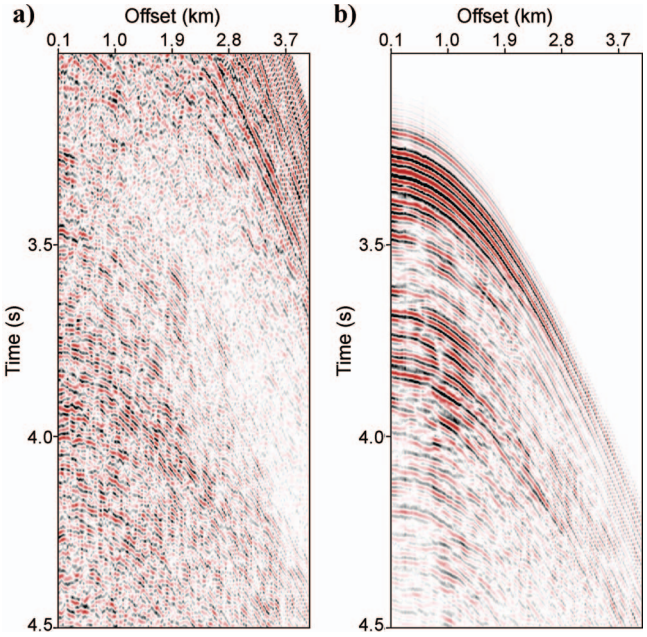

Figure 10. Center receiver lines from a 3D shot gather. (a) Data after free-surface multiple attenuation and (b) subtracted multiples.

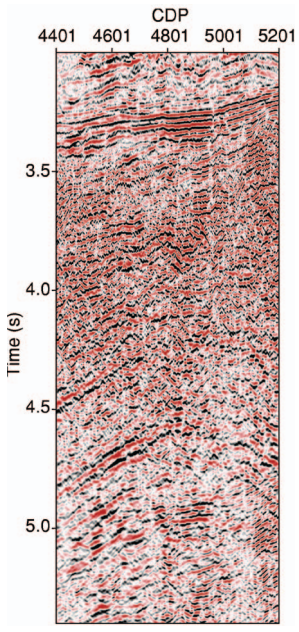

Figure 11. Poststack Kirchhoff time migration of the center receiver lines from the raw input data.

weighted least-squares problem introduced by the hyperbolic transform leads to large and sparse systems of equations in the time domain.

In this paper, we present an alternative numerical scheme based on parabolic sparse inversion. With a parabolic scheme, we solve many small systems of equations in the angular frequency domain. Solving many small systems is usually faster than solving a few big ones. This parallels the superior numerical efficiency of the parabolic Radon transform, compared to the hyperbolic transform of Thorson and Claerbout (1985). In our case, the dimension of the data vector, per frequency, equals the number of receiver cables or the number of coincident source and receiver lines, depending on details of the implementation. The dimension of the model space is several hundred. Hence, we solve a large number of underdetermined problems, for which it is appropriate to compute a minimum norm solution (Menke, 1989).

The parabolic approximation is acceptable when the maximum crossline offset is small compared to the target depth. This is usually fulfilled in 3D surface seismic acquisition. It may, however, be inadequate in an extension of 3D SRME to ocean-bottom seismic (OBS) data. The parabolic equation is a second-order Taylor-series approximation to the hyperbolic traveltime equation. In principle, higher-order (e.g., fourth-order) terms can be added, but this possibility has not been investigated.

The major advantage of the frequency-domain scheme is numerical efficiency. Different from a time-domain scheme, it does not have the ability to impose sparseness in the time direction, as demonstrated by Schonewille et al. (2004). Hence, we sacrifice some accuracy to achieve numerical efficiency. Using the proposed 3D SRME scheme, large-scale production processing becomes feasible. The computational cost is comparable to that of 3D prestack depth migration. Using a new cluster implementation of the method, running on 50 Linux processors with 3.06-GHz clock frequency, 3D multiple prediction for one sail line (1261 shots, eight receiver cables, 244 receivers per cable, 2048 samples per trace, 1024 frequencies, five to seven multiple contributions per trace, 660 model parameters) was timed to 32 hours elapsed time, or approximately 0.05 s per output trace. On a cluster with 1024 processors and with standard acquisition geometry, this corresponds to a throughput of approximately 175 km^2 perday.

The numerical examples show that the proposed 3D SRME scheme improves the multiple attenuation compared to 2D SRME for both synthetic and real data. In the Gauss-Cauchy sparse inversion, the regularization imposed by the Cauchy distribution of the prior is important to achieve this. The Gauss-Gauss solution, corresponding to the first iteration of the sparse inversion, does not give satisfactory results. This is in agreement with the results reported by van Dedem and Verschuur (2001, 2005). In numerical tests, we found that the best result was obtained using five iterations of sparse inversion. Increasing the number of iterations beyond this degraded the result.

In the deep water West Africa example presented above, the data were acquired with four receiver cables separated by 100 m, conventional flip-flop shooting, and 200-m sail-line separation. The nominal geometry corresponds to a source line almost coincident with each receiver line (Figure 8). Hence, a study of the receiver-line problem exclusively, without addressing the source-line separation problem, can be justified for this data set (van Borselen and Verschuur, 2003). In the NMO stack and poststack migration of the data, we dropped extrapolated small-offset traces and included maximum 3.0-km offset. For larger offsets, inaccurate multiple predictions caused by cable feathering degrades the performance of SRME.

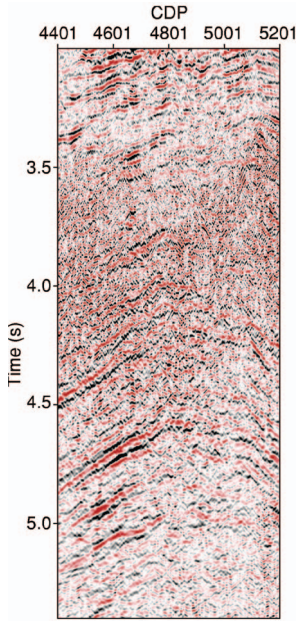

Figure 12. Poststack Kirchhoff time migration of the center receiver lines after 3D SRME.

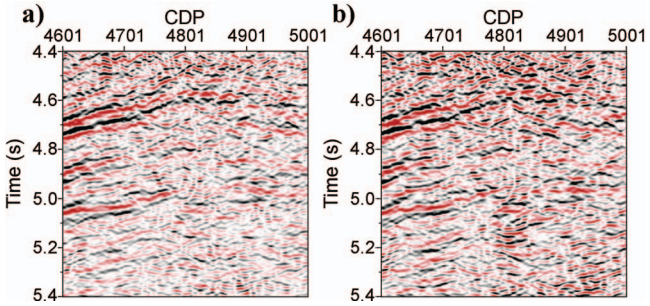

Figure 13. Poststack Kirchhoff time migration of the center receiver lines after (a) 3D SRME and (b) 2D SRME.

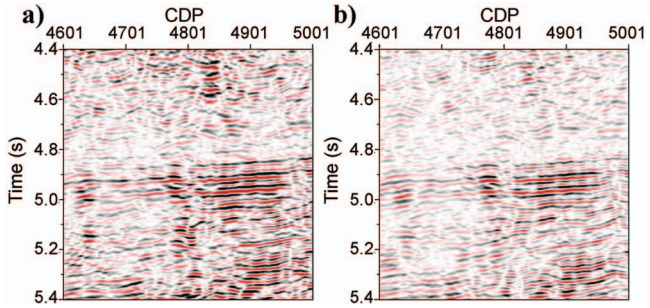

Figure 14. Poststack Kirchhoff time migration of the subtracted multiples after (a) 3D SRME and (b) 2D SRME.

DOI:10.1190/1.2345050

CONCLUSIONS

One of the main challenges in extension of SRME to 3D surface seismic data is coping with spatial aliasing because of the large distance between receiver cables. Here, we propose a solution to this, based on parabolic sparse inversion in the crossline direction. The parabolic sparse inversion problem can be solved efficiently in the frequency domain, such that production-scale processing of 3D seismic data sets is feasible on massive Linux clusters. Numerical results demonstrate that the proposed 3D SRME scheme gives improved results compared to 2D SRME for both synthetic and real data.

ACKNOWLEDGMENTS

We thank Statoil for permission to publish this work and the license partners Statoil and Chevron Texaco for permission to use the real data. We thank John Reidar Granli, Are Osen, Tage Røsten, Anders Sollid, and Eric Verschuur for helpful support and discussions. We also thank Mauricio D. Sacchi and two anonymous reviewers for comments and suggestions that improved the manuscript.

REFERENCES

Berkhout, A. J., 1982, Seismic migration: Imaging of acoustic energy by wave field extrapolation, A: Theoretical aspects: Developments in Solid Earth Geophysics, vol. 14A: Elsevier Science Publishing Co., Inc.

Berkhout, A. J., and D. J. Verschuur, 1997, Estimation of multiple scattering by iterative inversion, Part I: Theoretical considerations: Geophysics, **62**, 1586–1595.

Biersteker, J., 2001, MAGIC: Shell's surface multiple attenuation technique: 71st Annual International Meeting, SEG, Expanded Abstracts, 1301–1304.

Carvalho, P. M., A. B. Weglein, and R. H. Stolt, 1991, Examples of a nonlinear inversion method based on the *t*-matrix of scattering theory: Application to multiple suppression: 61st Annual International Meeting, SEG, Expanded Abstracts, 1319–1322.

Dragoset, W. H., and Z. Jericevic, 1998, Some remarks on surface multiple attenuation: Geophysics, **63**, 772–789.

Fokkema, J. T., and P. M. van den Berg, 1990, Removal of surface-related wave phenomena: The marine case: 59th Annual International Meeting, SEG, Expanded Abstracts, 1689–1692.

Hampson, D., 1986, Inverse velocity stacking for multiple elimination: Journal of the Canadian Society of Exploration Geophysics, **22**, 44–55.

Herrmann, P., T. Mojesky, M. Magesan, and P. Huginnet, 2000, De-aliased high-resolution Radon transforms: 70th Annual International Meeting, SEG, Expanded Abstracts, 1953–1956.

Hokstad, K., and R. Sollie, 2003, 3-D surface-related multiple elimination with parabolic sparse inversion: 73rd Annual International Meeting, SEG, Expanded Abstracts, 1961–1964.

———, 2004, 3-D surface-related multiple elimination with source-line reconstruction: 74th Annual International Meeting, SEG, Expanded Abstracts, 1261–1264.

Kennett, B. L. N., 1979, The suppression of surface multiples on seismic records: Geophysical Prospecting, **27**, 584–600.

Kleemeyer, G., S. E. Pettersson, R. Eppenga, C. J. Haneveld, J. Biersteker, and R. den Ouden, 2003, It's magic — Industry first 3D surface multiple elimination and pre-stack depth migration on Ormen Lange: 65th Annual International Meeting, EAGE, Extended Abstracts, B43.

Menke, W., 1989, Geophysical data analysis: Discrete inverse theory: Academic Press, Inc.

Sacchi, M. D., and T. J. Ulrych, 1995, High-resolution velocity gathers and offset space reconstruction: Geophysics, **60**, 1169–1177.

Sacchi, M. D., T. J. Ulrych, and C. J. Walker, 1998, Interpolation and extrapolation using a high-resolution discrete Fourier transform: IEEE Transactions on Signal Processing, **46**, 31–38.

Schonewille, M. A., and A. J. W. Duijndam, 2001, Parabolic Radon transform, sampling and efficiency: Geophysics, **66**, 667–678.

Schonewille, M., R. Hegge, and R. van Borselen, 2004, Sparse inversion techniques for 3-D SRME: Frequency or time domain?: 74th Annual International Meeting, SEG, Expanded Abstracts, 1265–1268.

Schonewille, M., and P. Zwartjes, 2002, High-resolution transforms and amplitude preservation: 72nd Annual International Meeting, SEG, Expanded Abstracts, 2066–2069.

Thorson, J. R., and J. F. Claerbout, 1985, Velocity-stack and slant-stack stochastic inversion: Geophysics, **50**, 2727–2741.

Ulrych, T. J., M. D. Sacchi, and A. Woodbury, 2001, A Bayes tour of inversion: A tutorial: Geophysics, **66**, 55–69.

van Borselen, R. G., J. T. Fokkema, and P. M. van den Berg, 1996, Removal of surface-related wave phenomena — The marine case: Geophysics, **61**, 202–210.

van Borselen, R., and D. J. Verschuur, 2003, Optimization of marine data acquisition for the application of 3D SRME: 73rd Annual International Meeting, SEG, Expanded Abstracts, 1965–1968.

van Dedem, E. J., and D. J. Verschuur, 2001, 3-D surface multiple prediction using sparse inversion: 71st Annual International Meeting, SEG, Expanded Abstracts, 1285–1288.

———, 2005, Surface-related multiple prediction: A sparse inversion approach: Geophysics, **70**, V31–V43.

Verschuur, D. J., A. J. Berkhout, and C. P. A. Wapenaar, 1992, Adaptive surface-related multiple elimination: Geophysics, **57**, 1166–1177.